Control Force Compensation in Ground-Based Flight Simulators

William W. Chung*
American Systems Corporation, NASA Ames Research Center, Moffett Field, CA, 94035

Peter M. T. Zaal† and Lorenzo Terenzi‡
San Jose State University, NASA Ames Research Center, Moffett Field, CA, 94035

Emily K. Lewis§
Metis Technology Solutions, NASA Ames Research Center, Moffett Field, CA, 94035

Matthew L. Blanken¶
NASA Ames Research Center, Moffett Field, CA, 94035

This paper presents the results of a study that investigated if controller force compensations accounting for the inertial forces and moments due to the aircraft motion during flight have a significant effect on pilot control behavior and performance. Seven rotorcraft pilots performed a side-step and precision hovering task in light turbulence in the Vertical Motion Simulator. The effects of force compensation were examined for two different simulated rotorcraft: linear and UH-60 dynamics with two different force gradients of the lateral stick control. Four motion configurations were used: large motion, hexapod motion, fixed-base motion, and fixed-base motion with compensation. Control-input variables and task performance, such as the time to translate to the designated hover position, station-keeping position errors, and handling qualities ratings, were used as measures. Control force compensation enabled pilot control behavior and performance more similar to that under high- or medium-fidelity motion to some extent only. Control force compensation did not improve overall task performance considering both rotorcraft models at the same time. The control force compensation had effects on the linear model with lighter force gradient, but only a minimal effect on pilots' control behavior and task performance for the UH-60 model, which had a higher force gradient. This suggests that the control force compensation has limited benefits for controllers that have higher stiffness.

I. Nomenclature

ϕ,$\dot{\phi}$,$\ddot{\phi}$	=	Roll attitude, rate, and acceleration of simulated rotorcraft
ϕ_{a_y},$\dot{\phi}_{a_y}$,$\ddot{\phi}_{a_y}$	=	Roll attitude, rate, and acceleration of the lateral stick due to inertia effect of lateral acceleration
Φ_{a_y}	=	Lateral stick displacement compensation due to lateral acceleration
Φ_c	=	Combined lateral stick displacement compensation due to inertial force and torque
ϕ_{pbd},$\dot{\phi}_{pbd}$,$\ddot{\phi}_{pbd}$	=	Roll attitude, rate, and acceleration of the lateral stick due to inertia effect of roll angular acceleration
Φ_{pbd}	=	Lateral stick displacement compensation due to roll angular acceleration
ω_{cf}	=	Cut-off frequency of pilot's lateral stick input
ω_n	=	Natural frequency of the lateral stick
ζ_y	=	Damping ratio of the lateral stick

*Principal Aerospace Engineer, Engineering and Analytical Solution Directorate, NASA Ames Research Center, Moffett Field, CA, 94035; william.w.chung@nasa.gov. Senior Member AIAA.

†Senior Research Engineer, Human Systems Integration Division, NASA Ames Research Center, Moffett Field, CA, 94035; peter.m.t.zaal@nasa.gov. Senior Member AIAA.

‡Research Scholar, Human Systems Integration Division, NASA Ames Research Center, Moffett Field, CA, 94035, and MSc. Student, Control and Simulation Division, Faculty of Aerospace Engineering, Delft University of Technology, Delft, Netherlands; lorenzo.terenzi@nasa.gov.

§Simulation Engineer Principal, SimLabs, NASA Ames Research Center, Moffett Field, CA, 94035; emily.k.lewis@nasa.gov.

¶Aerospace Engineer, Aerospace Simulation Research and Development, NASA Ames Research Center, Moffett Field, CA, 94035; matthew.l.blanken@nasa.gov. Senior Member AIAA.

a_y	=	Lateral acceleration at the lateral stick's pivot point of the simulated rotorcraft in body frame
g	=	Gravitational acceleration constant
I_{xx}	=	Moment of inertia about the pivot point of the lateral stick about the roll rotational axis
k_y	=	Force gradient of the lateral stick
l_c	=	Length of the lateral stick
m_c	=	Mass of the lateral stick
p or p_b	=	Roll angular rate of the simulated rotorcraft
$\dot{p}_b$	=	Roll angular acceleration of the simulated rotorcraft
r_c	=	Distance between the pivot point of the stick and the c.g. of the lateral stick
RMS	=	Root mean square
SK	=	Station-keeping score
sk	=	Station-keeping phase of the task
t_g	=	Time-to-target in the translation phase of the task
$trans$	=	Translational phase of the task
u	=	Lateral stick input
v	=	Lateral velocity of the simulated rotorcraft
$\dot{v}$	=	Lateral acceleration of the simulated rotorcraft
ye	=	Lateral position error

II. Introduction

While flying simulated vehicles, pilots adapt to different stimuli provided in a simulator, e.g., out-the-window visual, audio, motion, and hand-controller force feedback, depending on the task or maneuver. Timely motion feedback through the motion platform, as well as feedback from the force-feel system, can provide lead compensation in closed-loop control tasks and improve handling qualities and task performance [1–5]. Force-feel characteristics, such as the breakout, dead-band, damping, force gradient, and inertia of the controller all play an important role in the handling qualities of a (simulated) rotorcraft. Previous research focused on cyclic inceptor force-feel characteristics for improved handling qualities for both passive and active controllers [6–8].

Different from previous investigations, this study investigated haptic cues that are missing in fixed-base flight simulators that could contribute to tactile feedback pilots would have experienced otherwise in real flight. Specifically, this study focused on the inertial forces and moments a cyclic inceptor experiences due to the aircraft's motion that are either missing completely in fixed-base flight simulators, or being attenuated due to the application of washout filters in motion-based simulators. In an experiment conducted in the Vertical Motion Simulator (VMS) at NASA Ames Research Center, the effects on task performance, control behavior, and handling qualities ratings were investigated when restoring these reaction forces in fixed-base flight simulators.

The paper is structured as follows: Section III mathematically derives the control force compensation missing in fixed-base simulation. Section IV provides an overview of the experiment setup, including verification of the dynamic models, and the experimental hypotheses. The results are presented in Section V and discussed in Section VI. Finally, conclusions are provided in Section VII.

III. Control Force Compensation

The inertial force from the dynamics of the simulated rotorcraft's lateral acceleration, a_y, and roll angular acceleration, $\dot{p}_b$, Fig. 1a, are translated through the center control stick to the pilot as shown in Fig. 1b for the lateral and roll degrees-of-freedom.

The equations of motion of the lateral stick response due to the simulated rotorcraft's lateral and roll angular accelerations are described by Eqs. 1 and 2 as a function of control force-feel system damping, ζ_y, and force gradient, k_y.

$$I_{xx}\ddot{\phi}_{a_y} = -m_c a_y r_c - \zeta_y \dot{\phi}_{a_y} - k_y \phi_{a_y} \tag{1}$$

$$I_{xx}\ddot{\phi}_{pbd} = -I_{xx}\dot{p}_b - \zeta_y \dot{\phi}_{pbd} - k_y \phi_{pbd} \tag{2}$$

The lateral stick displacements, due to lateral accelerations, a_y, and angular accelerations, $\dot{p}_b$, are defined by Eqs. 3 and 4, respectively.

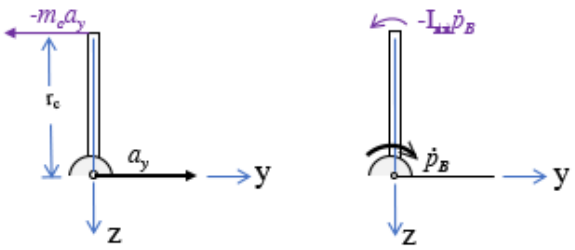

(a) The inertial force and torque acting on the mass center of the stick.

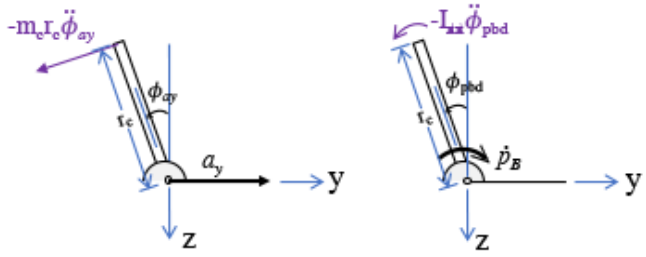

(b) Resulting stick displacement due to the inertial force and torque.

Fig. 1 Inertial forces acted on the stick due to simulated rotorcraft's dynamics.

$$\Phi_{a_y} = -\frac{m_c r_c}{I_{xx}} a_y \Big/ \left(s^2 + \frac{\zeta_y}{I_{xx}} s + \frac{k_y}{I_{xx}} \right) \tag{3}$$

$$\Phi_{pbd} = -\dot{p}_b \Big/ \left(s^2 + \frac{\zeta_y}{I_{xx}} s + \frac{k_y}{I_{xx}} \right) \tag{4}$$

The total compensation for the lateral control, Φ_c, or what is missing in a fixed-based simulation is the sum of these two dynamic components as shown in Eq. (5). Φ_c can be added to the control trim position to move the lateral stick in addition to pilot control inputs to simulate the stick force response due to the inertial force and moment from the rotorcraft's dynamics.

$$\Phi_c = \Phi_{a_y} + \Phi_{pbd} \tag{5}$$

IV. Experiment Setup

To investigate if control force compensation affects pilot control behavior and performance, a two degrees-of-freedom (DOF) lateral side-step task was developed in the VMS with the aim to compare results from no-motion conditions with and without control force compensation. The results were further compared with data from a near one-to-one motion condition, and a medium-fidelity motion condition representing motion found in typical hexapod motion simulators.

A. Rotorcraft Dynamics

A simulated linear 2-DOF rotorcraft model was adopted from previous work investigating the effects of roll-lateral motion on pilot performance [3]. The simulated rotorcraft model is provided in Eqs. 6 and 7.

$$\ddot{\phi} = -4.5\dot{\phi} + 1.7\delta_{lat} \tag{6}$$

$$\dot{v} = g \sin \phi \tag{7}$$

A second rotorcraft model, a full nonlinear UH-60 model [9] with a heavier force gradient of the lateral stick, was also used to investigate if there is a different effect from control force compensation depending on the controlled dynamics. For the UH-60, the Stability Augmentation System (SAS) was turned off purposely with an intent to force pilots to maintain close-loop stability. A comparison of the agility of the two rotorcraft models is shown in Fig. 2.

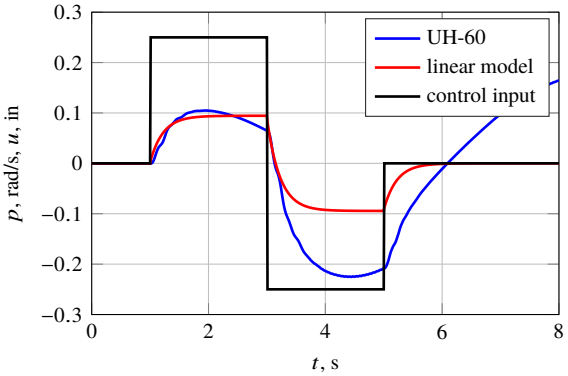

Fig. 2 Roll rate responses from both models from a lateral stick doublet.

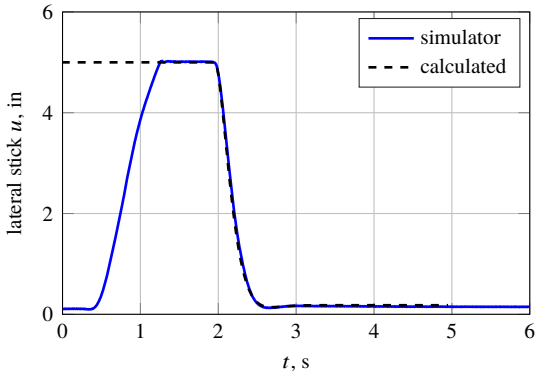

Fig. 3 Verification of mass properties in a pull-and-release test for the linear model.

B. Control Force-Feel System

To determine the mass and moment of inertia of the control stick in Eqs. 1-5, a pull test was conducted by setting the damping of the stick to zero and releasing the stick at its maximum lateral travel limit. The force gradient of the linear model was set to 0.6 lbf/in as in a previous test [3]. The resulting undamped natural frequency of the stick, ω_n, was measured at 1.194 Hz (or 7.5 rad/s). Using Eq. (1), with zero external force and zero damping based on a 25 inches rotational reference center for the particular control loader system, the moment of the inertia of the lateral stick was calculated from Eqs. 8 to be 2577 lbm-in about the lateral stick's rotational center. The effective damping ratio of the stick would come out to be 0.85. With these properties, the stick's lateral characteristics would be acceptable according to Ref. [8]. A check of the pull-release response of the measured moment inertia vs. the lateral stick response from the simulator is shown in Fig. 3.

$$\omega_n = \sqrt{k_y / I_{xx}} \quad \text{or} \quad I_{xx} = k_y / \omega_n^2 \tag{8}$$

The product of mass and the rotational center to the center of c.g. of the stick, $m_c r_c$ in Eq. (3), was estimated through an experimental process since it was difficult to disassemble the roll rotational assembly from the control loader system. The VMS was configured with near one-for-one motion by setting the second-order high-pass washout filter frequencies for both the roll and lateral degree of freedom (DOF) to 0.001 rad/s with a unity gain. A doublet of lateral acceleration was commanded to drive the motion system. By comparing the stick displacement response and the compensation model, $m_c r_c$, is estimated to be 52 $lb_m - in^2$. With this estimate, the resulted lateral stick displacement compensation shows a good match to the simulator response as shown in Fig. 4. The compensation due to a roll angular acceleration also shows a good match as shown in the same figure.

The lateral stick's control-force feel for the UH-60 had a breakout force of 1 lbf, a damping ratio of 0.722, and a force gradient of 1 lbf/in, which resulted an undamped natural frequency of 9.7 rad/s. This would also be acceptable according to Ref. [8].

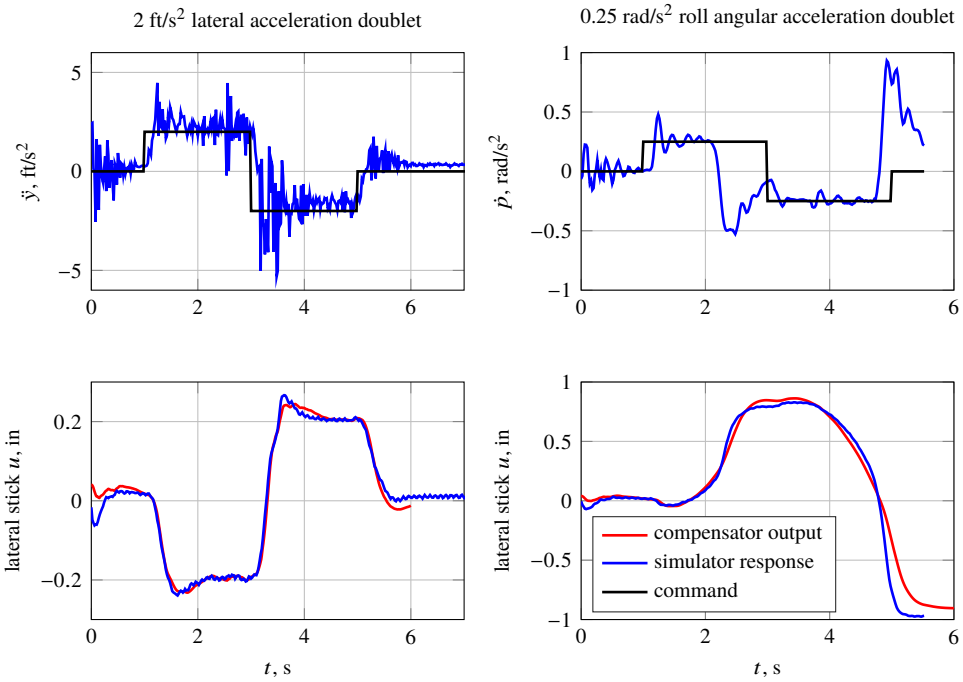

Fig. 4 Verification of the control force compensation for the lateral stick displacements.

C. Task

A 20-foot side-step task was developed to investigate the effect of the control force compensation to the stick due to the lateral accelerations and roll angular accelerations in ground-based flight simulators. Altitude hold, heading hold, as well as forward position hold were assumed to be active to limit the DOFs to roll and lateral only as defined by the model described in Eqs. 1 and 2.

All test participants were briefed on the test procedures and task performance criteria prior to taking the test. Test participants were instructed to initiate a smooth lateral input toward the station-keeping position 20 feet to the right in 5 seconds (or time-to-target) for desired performance, and 7 seconds for adequate performance. Once the simulated rotorcraft was visually within the desired station-keeping region, test participants were directed to maintain the station-keeping position in a light disturbance for 10 seconds. Desired, adequate, and not-adequate performance criteria for the station-keeping phase of the task were given to the test participants as shown in Fig. 5.

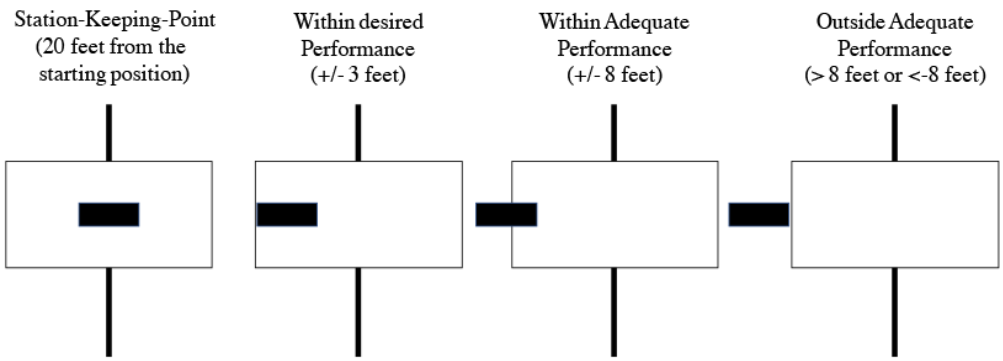

Fig. 5 Task performance criteria via a hover-target board in the out-the-window visual scene.

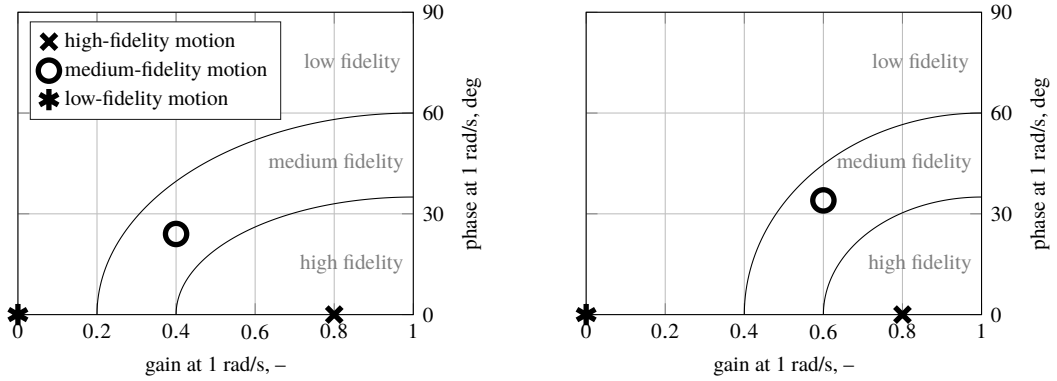

(a) Roll degree of freedom. **(b) Lateral degree of freedom.**

Fig. 6 Sinacori plots of the experimental conditions.

Table 1 Experimental conditions.

Condition	Rotorcraft Model	Motion Fidelity
1	linear model	high
2		medium
3		low
4		low + compensation
5	UH-60	high
6		medium
7		low
8		low + compensation

D. Conditions

To investigate the effect of inertial stick force compensation and its interaction with aircraft dynamics, the experiment had two independent variables: motion fidelity with four levels (high-fidelity, medium-fidelity, low-fidelity, and low-fidelity with compensation) and rotorcraft model with two levels (linear and UH-60 dynamics). The experiment had a full-factorial design resulting in eight experimental conditions. The motion configurations were plotted against the modified Sinacori motion fidelity criteria [3] are shown in Fig. 6. The motion gain for the high-fidelity configuration was reduced from unity to 0.8 to alleviate excessive lateral accelerations from the UH-60 model. The test matrix is shown in Table 1.

E. Participants and Procedures

Seven pilots participated in the experiment. All had extensive rotorcraft flying experience. Every pilot received an extensive briefing and safety-walk-around before the start of the experiment.

The original experiment was divided into two sessions. Each session tested the experimental conditions for one rotorcraft model. Training was provided to all test participants at the beginning of each session. Six simulated runs of each test configurations were given to test participants in random order. However, due to an error in the implementation of the control force compensation, the low-fidelity conditions were repeated by the seven test participants several weeks after the first trial of testing. During the second trial of testing, the low-fidelity conditions were presented randomly in two sessions as well. The two motion conditions were not repeated.

F. Apparatus

The VMS, Fig. 7a, with its large motion envelope provides the realistic cueing environment necessary for performing handling qualities studies, has an operational lateral travel of 30 feet. The simulator was positioned to the left-side of the

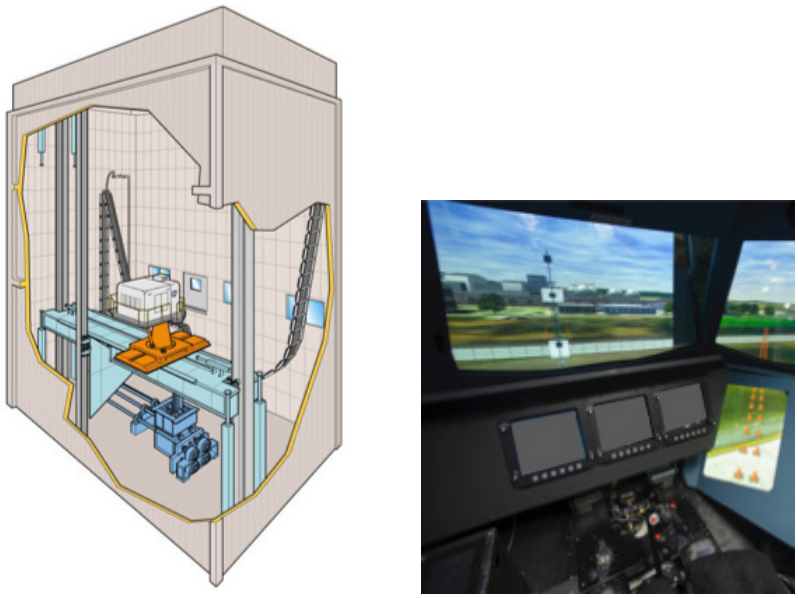

(a) Motion system. **(b) Cockpit.**

Fig. 7 The Vertical Motion Simulator at NASA Ames Research Center.

lateral travel, to have room for the 20-foot side-step task to the right for the high-fidelity motion configuration. On average, about 20 feet of lateral travel was used for the high-fidelity motion configuration, and about five feet of lateral travel was used for the medium-fidelity motion.

The rotorcraft cockpit had a cyclic control stick as shown in Fig. 7b. No instruments were used. Pilots did have an out-of-the-window view with a field-of-view (FOV) of 160 deg in azimuth and vertical FOV of 25 deg, plus a chin-window in a typical rotorcraft configuration. With this FOV, pilots would have the hover target in their view all the time from the beginning to the end of the side-step and station-keeping phases of the task.

G. Dependent Measures

The experiment considered two subjective handling qualities ratings (HQR) [10] as dependent measures: the HQR rating during the transnational phase of the task (HQR_{trans}) and the HQR rating during the station keeping phase (HQR_{sk}). These ratings were collected in separate runs for conditions 1, 3, and 4 only at the end of the experiment. The HQR were collected only for the linear model.

The following eight objective performance variables were considered as dependent measures: the time-to-target, t_g; the root mean square (RMS) of pilots' control inputs, RMS_u; the bandwidth of the control inputs, ω_{cf} [11]; the station keeping score, SK; the RMS of the lateral position and velocity during the station-keeping phase, RMS_{ye} and RMS_v; and the RMS of the roll angle and rate during the station-keeping phase, RMS_ϕ and RMS_p respectively.

The time-to-target, t_g, was the time between two button presses on the center stick. Pilots pressed the event button the first time when they were ready to start transitioning to the hover target. They pressed the button a second time when they felt they were within the desired hover bound and would likely stay in the desired area. Both ω_{cf} and RMS_u were calculated for the entire run, i.e., for both the translation and the station-keeping phases. The station-keeping score, SK, ranged from 1 to 3. A score of 1 was given to desired performance achieved during the station-keep phase of the task, 2 was given to adequate performance, and 3 was given to not-adequate performance (Fig. 5). The remaining objective measures (RMS_{ye}, RMS_v, RMS_ϕ, and RMS_p) were all calculated for the station-keeping phase only. The lateral position error, RMS_{ye}, was calculated relative to the center of the hover-target board (Fig. 5).

H. Hypotheses

The following hypotheses were formulated based on the characteristics of the control force compensation as derived in Section III and the controlled dynamics presented in Section IV.A:

H1: Since the control force compensation in the fixed-base condition is simulating the inertial force and moment feedback due to the motion of the simulated aircraft, it was expected that pilots performing the task with compensation would control more similarly to performing the task under medium-fidelity or high-fidelity motion compared to performing the task without compensation. This would be visible in ω_{cf} and RMS_u.

H2: As the control force compensation provides lead information similar to motion feedback, albeit less efficient, it was expected that the compensation would result in improved task performance compared to the fixed-base condition without compensation, i.e., a shorter time-to-target t_g; smaller RMS of the lateral position error RMS_{ye}, roll angle RMS_ϕ, lateral velocity RMS_v, and roll rate RMS_p during the station-keeping task; and a better station-keeping score SK.

H3: Since the higher force gradient of the UH-60 model would result in a smaller magnitude of force compensation at the stick, it was hypothesized that pilots controlling the UH-60 model would benefit less from the control force compensation as compared to the linear model, i.e., the performance improvement would be less for the UH-60 model compared to the linear model and control behavior would be more similar to the condition without compensation.

H4: It was expected that both high-fidelity and medium-fidelity motion would still provide larger improvements in pilot performance compared to both low-fidelity conditions, as motion provides faster lead information as compared to haptic feedback. Therefore, performance in the low-fidelity condition with compensation was expected to lie between performance in the medium-fidelity and low-fidelity-without-compensation conditions.

V. Results

In this section, the main results of the experiment and the associated data analysis are presented. The seven continuous dependent measures under consideration are: t_g, RMS_u, ω_{cf}, RMS_{ye}, RMS_v, RMS_ϕ, RMS_p. The three ordinary variables considered are the performance score SK and the HQR rating for the translation and station keeping phases, respectively. Table 2 and Table 3 present the means and standard deviations of the dependent measures for each condition with the exception of the HQR ratings, which deviated strongly from normality. Table 4 provides the means of the data collapsed over the rotorcraft models for the same dependent measures.

A. Ordinal Variables

1. HQR Ratings

The participants were asked to subjectively evaluate the handling qualities of the linear model using the Cooper Harper rating. They were asked to rate the translation and station keeping phase of the task separately (HQR_{trans} and HQR_{sk}, respectively). The assigned scores ranged from 1 to 10, with 1 indicating the best handling characteristics and 10 the worst [10]. The pilot responses are shown in Figs. 8a and 8b.

The Jonckheere trend test [12] was used to test the hypothesis that high-fidelity motion would receive the lowest scores, followed by the fixed-base condition with compensation, followed by the fixed base condition without compensation, in this order. The results of the test show a non-significant trend: $JT = 57$, $p = 0.1304$. Furthermore, a generalized linear model based on Generalized Estimating Equations (GEE based on logistic regression) was fit to the data, using

Table 2 Mean of the dependent measures.

Model	Fidelity	t_g	SK	RMS_u	ω_{cf}	RMS_{ye}	RMS_v	RMS_ϕ	RMS_p
Linear	High	4.779	1.333	0.401	4.072	1.544	1.401	3.138	0.104
UH-60	High	4.476	1.214	0.334	3.999	1.169	1.240	4.632	0.102
Linear	Medium	4.369	1.405	0.547	2.450	1.692	1.689	4.603	0.140
UH-60	Medium	4.392	1.286	0.332	3.072	1.394	1.375	5.110	0.113
Linear	Low+Comp	4.729	1.262	0.577	2.614	1.465	1.563	5.050	0.184
UH-60	Low+Comp	4.462	1.238	0.547	2.809	1.429	1.489	6.193	0.296
Linear	Low	4.698	1.429	0.591	2.153	1.970	1.959	5.981	0.195
UH-60	Low	4.502	1.286	0.532	2.758	1.434	1.476	6.185	0.195

Table 3 Standard deviation of the dependent measures.

Model	Fidelity	t_g	SK	RMS_u	ω_{cf}	RMS_{ye}	RMS_v	RMS_ϕ	RMS_p
Linear	High	0.736	0.473	0.104	0.698	0.587	0.485	0.855	0.027
UH-60	High	0.617	0.411	0.131	0.625	0.415	0.378	0.908	0.042
Linear	Medium	0.500	0.538	0.479	0.619	0.850	0.643	1.940	0.064
UH-60	Medium	0.445	0.453	0.150	0.750	0.653	0.565	1.478	0.053
Linear	Low+Comp	0.567	0.492	0.403	0.513	0.592	0.831	3.760	0.148
UH-60	Low+Comp	0.556	0.480	0.492	0.609	0.904	0.759	2.861	0.619
Linear	Low	0.984	0.542	0.416	0.435	1.018	0.964	4.095	0.143
UH-60	Low	0.513	0.453	0.488	0.678	0.686	0.860	3.495	0.181

Table 4 Mean aggregate value for fidelity.

Fidelity	t_g	SK	RMS_u	ω_{cf}	RMS_{ye}	RMS_v	RMS_ϕ	RMS_p
High	4.63	1.27	0.37	4.04	1.36	1.32	3.89	0.10
Medium	4.38	1.35	0.44	2.76	1.54	1.53	4.86	0.13
Low+Comp	4.60	1.25	0.56	2.71	1.45	1.53	5.62	0.24
Low	4.60	1.36	0.56	2.46	1.70	1.72	6.08	0.19

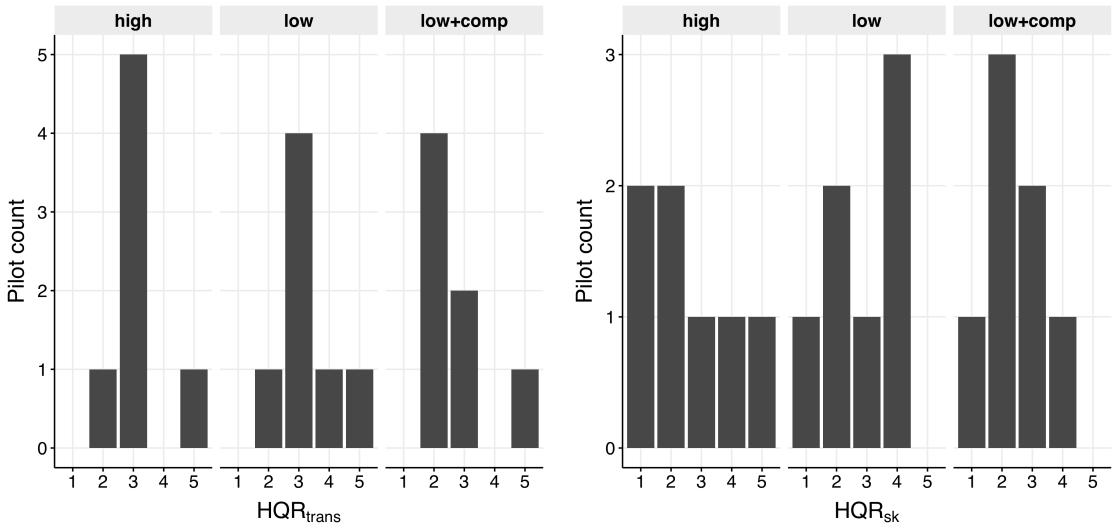

(a) Translation maneuver HQR. **(b) Station keeping HQR.**

Fig. 8 HQR rating given for the translation and station keeping phase of the task.

Table 5 HQR statistical test results.

	HQR_{trans}				HQR_{sk}			
	Estimate	Std.err	Wald	p	Estimate	Std.err	Wald	p
High Fidelity vs. Low	0.048	0.135	0.124	0.725	-0.024	0.198	0.014	0.904
Low Fidelity Without vs. With Comp	0.286	0.256	1.244	0.265	0.214	0.273	0.618	0.432

Table 6 Summary of aggregated HQR means and standard errors.

	HQR_{trans}		HQR_{sk}	
Fidelity	Mean	Std.err	Mean	Std.err
High	2.143	0.340	2.571	0.571
Low	2.285	0.359	2.857	0.459
Low+Comp.	1.714	0.420	2.428	0.369

the Gaussian family and as cluster variable the participant ID. The planned contrasts for the model compared the high fidelity case against the low-fidelity ones and the low-fidelity cases with and without compensation against each other.

For the variable HQR_{trans}, the first contrast shows that there is no significant difference between high-fidelity and (combined) low-fidelity conditions. The same holds for the difference between the low fidelity with compensation and without. For the variable HQR_{sk}, the first contrast shows that there is no significant difference between high-fidelity and (combined) low-fidelity conditions. The same hold for the difference between the low-fidelity with compensation and without. The full test results are shown in Table 5. The means and standard errors of the aggregated data are summarized in Table 6.

2. Station-Keeping Score, SK

The station-keeping score, or SK, ranged from 1 to 3. A score of 1 indicates desired performance during the station-keep phase of the task, 2 indicates adequate performance, and 3 indicates not-adequate performance as shown in Fig. 5. The data, aggregated over motion-fidelity and aircraft-model variables, are shown in histograms in Fig. 9. Since the data are ordinal and highly non-normal a generalized linear model based on Generalized Estimating Equations (GEE based on logistic regression) was fit to the data, using the Poisson family with logarithmic link function and as cluster variable the participant id. The summary of the statistical results derived from the model are shown in Table 7. The rotorcraft model suggestively affected the score; $b = -0.077$, $\chi^2 = 3.308, p = 0.069$. The mean SK rating for the UH-60 model ($M = 1.25$) was lower than for the linear model ($M = 1.35$).

B. Continuous Variables

For the continuous variables linear regression models were used for hypothesis testing, having as independent within-subject variables the simulation fidelity (Fidelity) and aircraft model (Model). First, a repeated-measures Analysis of variance (ANOVA) was conducted on the continuous variables. Unfortunately, most fidelity conditions violated the assumption of homogeneity of variances of the residuals. For this reason, a linear mixed-effect model was fit for all the continuous variables since it does not assume homogeneity of variances of the residuals and can account for the residual dependency by using the pilot ID as a random factor [13]. Adding pilot ID as the random factor significantly improved every model that is discussed further. To compare specific conditions without correcting for multiple comparisons, orthogonal constants where used [14]. The orthogonal contrasts considered were the same for all the conditions:

1) High fidelity vs. others compares the mean of the high-fidelity against the aggregate mean of the all the other conditions.
2) Medium fidelity vs. low compares the mean of the medium-fidelity condition against the aggregate mean of both the low-fidelity conditions.
3) Low fidelity with vs. without compensation compares the mean of the low-fidelity condition with and without compensation.

The analysis of variance test results are summarized in Table 8. The overall effect sizes are tabulated in Table 9 to

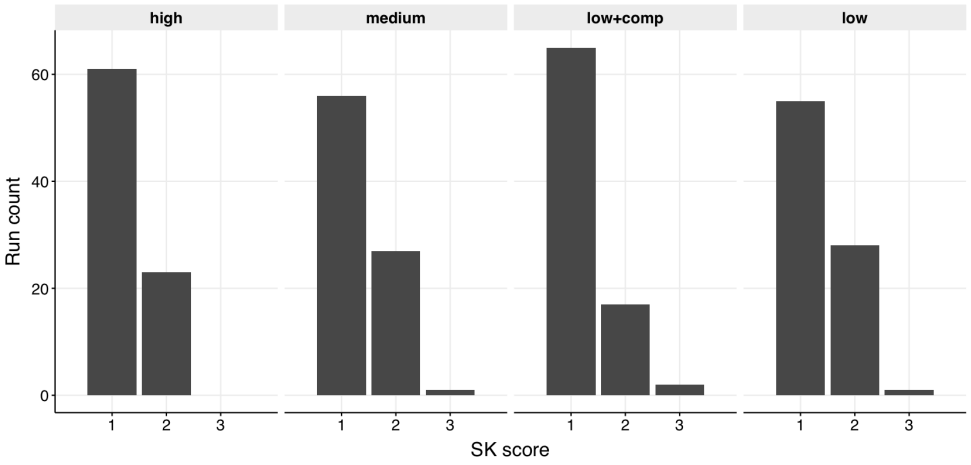

(a) SK score per fidelity level.

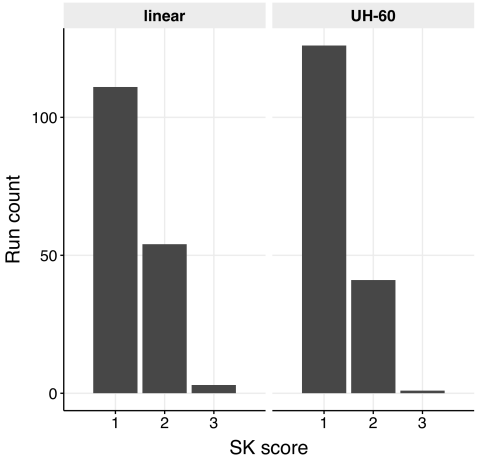

(b) Sk score per aircraft model.

Fig. 9 Station Keeping scores.

Table 7 Summary of statistical results for the station keeping score.

	Estimate	Std.err	Wald	p
Model	-0.077	0.042	3.308	0.069
High Fidelity vs. Others	-0.006	0.017	0.100	0.752
Medium Fidelity vs. Low	0.015	0.018	0.727	0.394
Low Fidelity Without vs. With Comp	-0.062	0.051	1.493	0.222
Model × High Fidelity vs. Others	-0.006	0.020	0.081	0.775
Model × Medium Fidelity vs. Low	-0.009	0.014	0.394	0.530
Model × Low Fidelity Without vs. With Comp	0.043	0.059	0.534	0.465

= significant ($p \leq 0.05$)

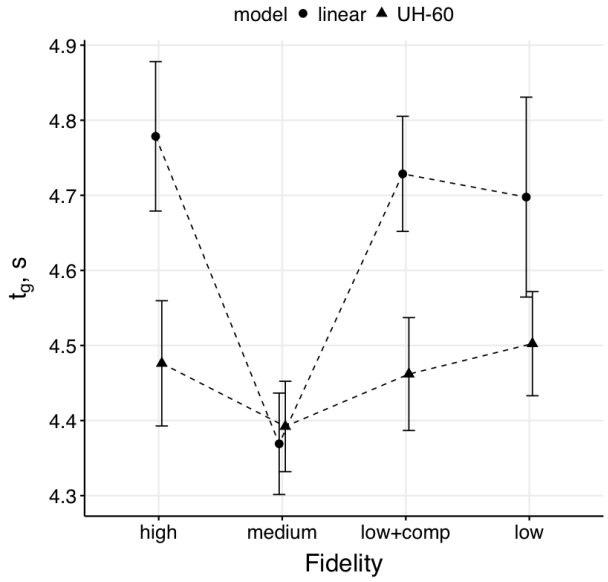

(a) Time to target.

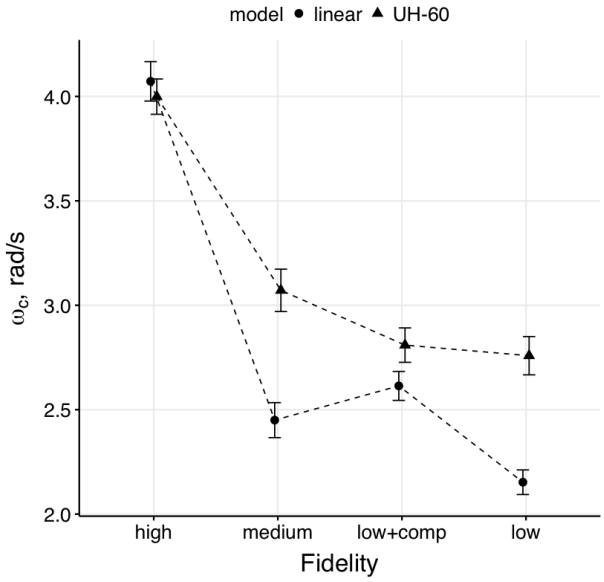

(b) Control input cut-off frequency.

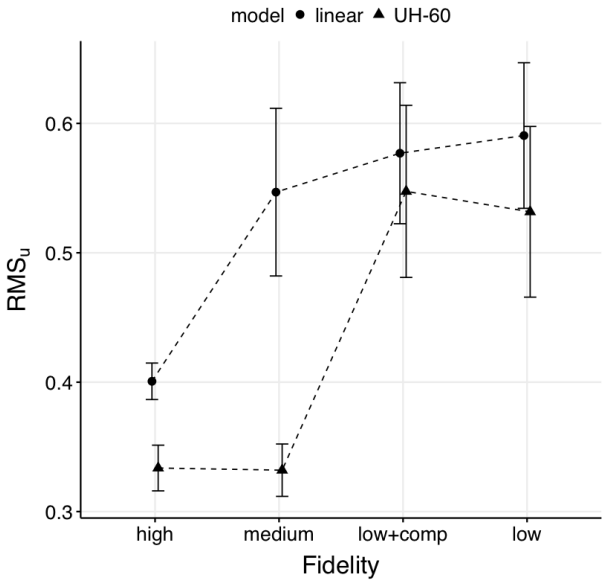

(c) RMS control input.

Fig. 10 Time to target and control input depended measures.

Table 14, and represented graphically in Figs. 10 and 11.

1. Time-to-Target, t_g

The error-bar plot of the time-to-target for each of the conditions can be seen in Fig. 10a. The summary of the linear mixed effect model is provided in Table 9. The different aircraft models did not have a significant effect on the time-to-target. The time-to-target was significantly lower between the medium-fidelity (M = 4.38) and the low-fidelity conditions (M = 4.6 s); $b = -0.115$ (SE = 0.048), $t(29.3) = -2.401$, $p = 0.023$.

Table 8 Type III Analysis of Variance Table with Satterthwaite's method for the Multilevel Models

Measure	Model			Fidelity			Model × Fidelity		
	df	*F*	*p*	*df*	*F*	*p*	*df*	*F*	*p*
t_g	1,6	1.9056	0.2167	3, 18	1.2921	0.3075	3, 18	1.4894	0.2511
RMS_u	1,6	7.528	0.0336	3, 18	2.015	0.148	3, 18	2.164	0.128
ω_{cf}	1, 6	6.318	0.0457	3, 18	27.59	< 0.001	3, 18	5.013	0.011
RMS_{ye}	1,6	10.23	0.0186	3,18	2.286	0.113	3,18	1.352	0.289
RMS_v	1, 6	11.9	0.014	3, 18	1.636	0.216	3, 18	2.415	0.100
RMS_ϕ	1, 6	14.365	0.009	3, 18	3.388	0.041	3, 18	4.489	0.016
RMS_p	1,6	0.593	0.471	3, 18	4.326	0.01836	3, 18	1.469	0.256

= significant ($p \leq 0.05$)

Table 9 Summary of the mixed effect model fitted for the time-to-target.

	Estimate	Std. Error	df	t value	p
Model	-0.185	0.134	5.999	-1.380	0.217
High Fidelity vs. Others	0.045	0.034	29.302	1.333	0.193
Medium Fidelity vs. Low	-0.115	0.048	29.302	-2.401	0.023
Low Fidelity Without vs. With Comp	0.015	0.083	29.302	0.187	0.853
Model × High Fidelity vs. Others	-0.039	0.035	17.998	-1.131	0.273
Model × Medium Fidelity vs. Low	0.085	0.049	17.998	1.735	0.100
Model × Low Fidelity Without vs. With Comp	-0.036	0.085	17.998	-0.422	0.678

= significant ($p \leq 0.05$)

2. Cut-Off Frequency, ω_{cf}

The error-bar plot Of the control input cut-off frequency for each of the conditions can be seen in Fig. 10b. The summary of the linear mixed-effect model is shown in Table 10. There was a significant interaction effect between the rotorcraft model type and the high-fidelity vs. other contrast; $b = -0.137$ (SE = 0.044), $t(18) = -3.146$, $p = 0.006$. As can be seen in Fig. 10b at low- and medium-fidelity conditions, the cut-off frequency for the UH-60 was systematically higher than the one for the linear model while for the high fidelity case this difference disappeared. The cut-off frequency was significantly higher with high-fidelity compared to the other conditions; $b = 0.417$ (SE = 0.045), $t(28, 22) = 9.336$, $p < 0.001$. Moreover, the cut-off frequency for the low-fidelity condition with compensation ($M = 2.71$ rad/s) was significantly higher than the one for the low fidelity condition without compensation ($M = 2.46$ rad/s); $b = 0.231$ (SE = 0.109), $t(18) = -3.146$, $p = 0.044$.

3. RMS Control Input, RMS_u

The error-bar plot of time-to-target for each of the conditions is depicted in Fig. 10c. The summary of the linear mixed effect model is shown in Table 11. There was a significant interaction between the aircraft model and the medium- vs. low-fidelity conditions; $b = -0.057$ (SE = 0.023), $t(18) = -2.466$, $p = 0.024$. Even in presence of an interaction, the overall mean of the RMS_u for the linear model ($M = 0.529$) was significantly higher than the one for the UH-60 ($M = 0.436$); $b = -0.093$ (SE = 0.034), $t(6) = -2.744$, $p = 0.034$. The RMS_u for the high-fidelity case ($M = 0.37$) is lower than the one for the medium ($M = 0.44$) and low fidelity cases ($M = 0.56$), although the effect is not significant, $p = 0.055$.

Table 10 Summary of the mixed effect model fitted to the cut-off frequency.

	Estimate	Std. Error	df	t value	p
Model	0.337	0.134	6.000	2.514	0.046
High Fidelity vs. Others	0.417	0.045	28.225	9.336	< 0.001
Medium Fidelity vs. Low	0.022	0.063	28.225	0.352	0.727
Low Fidelity Without vs. With Comp	0.231	0.109	28.225	2.109	0.044
Model × High Fidelity vs. Others	-0.137	0.044	18.000	-3.146	0.006
Model × Medium Fidelity vs. Low	0.074	0.062	18.000	1.197	0.247
Model × Low Fidelity Without vs. With Comp	-0.205	0.107	18.000	-1.926	0.070

= significant ($p \leq 0.05$)

Table 11 Summary of the mixed effect model fitted to the RMS of the control input.

	Estimate	Std. Error	df	t value	p
Model	-0.093	0.034	6.000	-2.744	0.034
High Fidelity vs. Others	-0.043	0.021	24.090	-2.017	0.055
Medium Fidelity vs. Low	-0.012	0.030	24.090	-0.411	0.685
Low Fidelity Without vs. With Comp	-0.007	0.052	24.090	-0.132	0.896
Model × High Fidelity vs. Others	0.009	0.016	17.999	0.522	0.608
Model × Medium Fidelity vs. Low	-0.057	0.023	17.999	-2.466	0.024
Model × Low Fidelity Without vs. With Comp	0.015	0.040	17.999	0.369	0.717

= significant ($p \leq 0.05$)

Table 12 Summary of the mixed effect model fitted for the RMS of the lateral position error.

	Estimate	Std. Error	df	t value	p
Model	-0.311	0.097	5.948	-3.208	0.019
High Fidelity vs. Others	-0.041	0.038	35.628	-1.080	0.288
Medium Fidelity vs. Low	-0.009	0.054	35.628	-0.159	0.875
Low Fidelity Without vs. With Comp	-0.252	0.094	35.628	-2.691	0.011
Model × High Fidelity vs. Others	-0.021	0.052	17.910	-0.407	0.689
Model × Medium Fidelity vs. Low	-0.004	0.073	17.910	-0.056	0.956
Model × Low Fidelity Without vs. With Comp	0.250	0.127	17.910	1.971	0.064

= significant ($p \leq 0.05$)

4. RMS Lateral Position Error, RMS_{ye}

The error-bar plot of the RMS lateral position error for each of the conditions can be seen in Fig. 11a. The summary of the linear mixed effect model is provided in Table 12. The RMS_{ye} for the linear model ($M = 1.66$) was significantly higher than the RMS_{ye} for the UH-60 model ($M = 1.33$); $b = -0.311$ (SE = 0.038), $t(5.94) = -3.2$, $p = 0.019$. Furthermore, the statistical analysis reveals that the mean RMS_{ye} of low fidelity with compensation ($M = 1.45$) was significantly lower than the one of the same fidelity but without compensation ($M = 1.7$); $b = -0.0252$ (SE = 0.094), $t(35.62) = -2.691$, $p = 0.011$. Indeed, for the UH-60 the means for the low fidelity case with ($M = 1.429$) and without compensation ($M = 1.434$) were quite similar. On the other hand, for the linear case the means for the low fidelity case with ($M = 1.465$) and without compensation ($M = 1.970$) showed a difference.

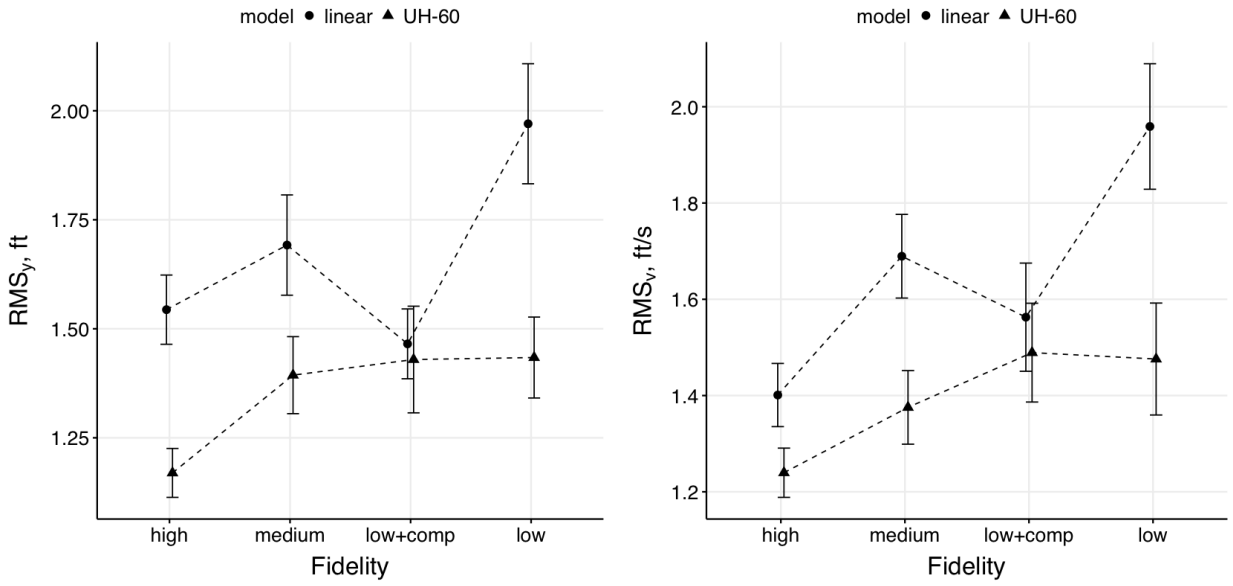

(a) RMS lateral error.

(b) RMS lateral velocity.

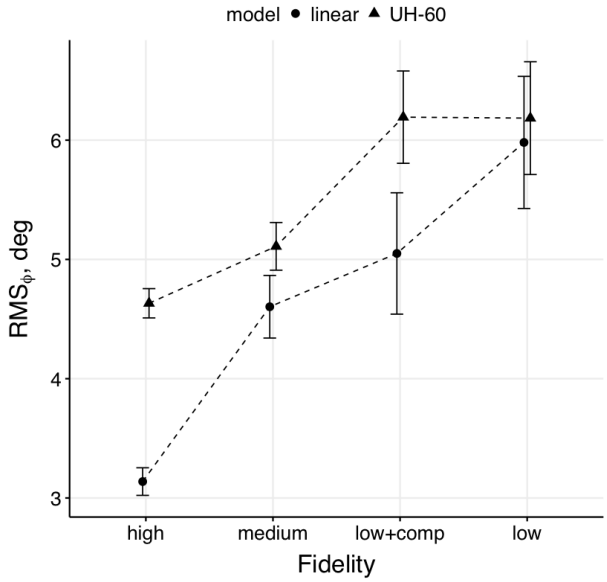

(c) RMS roll attitude.

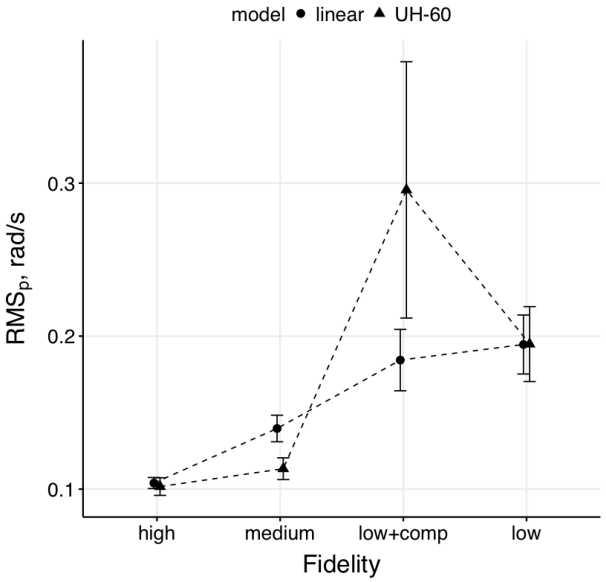

(d) RMS roll rate.

Fig. 11 Lateral and roll performance depended measures.

5. RMS Lateral Velocity, RMS_v

The error-bar plot of the RMS lateral velocity for each of the conditions can be seen in Fig. 11b. The summary of the linear mixed effect model is shown in Table 13. RMS_v for the UH-60 ($M = 1.39$) was significantly lower than the RMS_v of the linear model ($M = 1.65$); $b = -0.258$ (SE = 0.075), $t(6) = -3.450$, $p = 0.014$. Furthermore, the RMS_v was significantly lower for the high-fidelity condition compared to the rest of the conditions; $b = -0.084$ (SE = 0.04), $t(25.198) = -2.087$, $p = 0.047$. There was a significant interaction between the model type and the low fidelity conditions; $b = 0.205$ (SE = 0.082), $t(18) = 2.500$, $p = 0.022$. The biggest effect of the force compensation algorithm is observed for the linear model.

Table 13 Summary of the mixed effect model fitted for the RMS of the lateral velocity.

	Estimate	Std. Error	df	t value	p
Model	-0.258	0.075	5.996	-3.450	0.014
High Fidelity vs. Others	-0.084	0.040	25.198	-2.087	0.047
Medium Fidelity vs. Low	-0.024	0.057	25.1.98	-0.419	0.679
Low Fidelity Without vs. With Comp	-0.198	0.099	25.198	-2.009	0.055
Model × High Fidelity vs. Others	0.032	0.033	18.000	0.964	0.348
Model × Medium Fidelity vs. Low	-0.012	0.047	18.000	-0.251	0.804
Model × Low Fidelity Without vs. With Comp	0.205	0.082	18.000	2.500	0.022

= significant ($p \leq 0.05$)

6. RMS Roll Attitude, RMS_ϕ

The error-bar plot of the RMS roll attitude for each of the conditions can be seen in Fig. 11c. The summary of the linear mixed effect model is provided in Table 14. There was a significant interaction between the model type in the contrast of the high-fidelity condition against the other conditions; $b = 0.219$ (SE = 0.0), $t(20.53) = 2.738$, $p = 0.014$. Furthermore the model significantly interacted between the low-fidelity condition with (for the linear model $M = 5.05$ and for the UH-60 $M = 6.19$)) and without compensation (for the linear model $M = 5.98$ and for the UH-60 $M = 6.185$); $b = 0.470$ (SE = 0.196), $t(18) = 2.394$, $p = 0.028$.

Table 14 Summary of the mixed effect model fitted for the RMS of the roll angle.

	Estimate	Std. Error	df	t value	p
Model	0.837	0.221	6.020	3.790	0.009
High Fidelity vs. Others	-0.518	0.156	20.543	-3.323	0.003
Medium Fidelity vs. Low	-0.304	0.221	20.543	-1.378	0.183
Low Fidelity Without vs. With Comp	-0.465	0.382	20.543	-1.218	0.237
Model × High Fidelity vs. Others	0.219	0.080	17.995	2.738	0.014
Model × Medium Fidelity vs. Low	-0.056	0.113	17.995	-0.491	0.629
Model × Low Fidelity Without vs. With Comp	0.470	0.196	17.995	2.394	0.028

= significant ($p \leq 0.05$)

7. RMS Roll Rate, RMS_p

The error-bar plot of the RMS roll rate for each of the conditions is provided in Fig. 11d. The summary of the linear mixed effect model is shown in Table 15. No significant effects were detected for this variable.

Table 15 Summary of the mixed effect model fitted for the RMS of the roll rate.

	Estimate	Std. Error	df	t value	p
Model	0.021	0.027	5.998	0.770	0.470
High Fidelity vs. Others	-0.017	0.011	34.958	-1.512	0.139
Medium Fidelity vs. Low	-0.017	0.016	34.958	-1.031	0.310
Low Fidelity Without vs. With Comp	-0.005	0.028	34.958	-0.183	0.856
Model × High Fidelity vs. Others	-0.008	0.015	17.993	-0.524	0.607
Model × Medium Fidelity vs. Low	-0.027	0.021	17.993	-1.321	0.203
Model × Low Fidelity Without vs. With Comp	0.055	0.036	17.993	1.546	0.139

VI. Discussion

The purpose of this study was to investigate if control force compensation affects pilot control behavior and performance. Therefore, the main goal was comparing the low-fidelity condition with and without compensation to assess the benefit, if any, of the force feedback algorithm. The high- and medium-fidelity conditions were used as baselines for the low-fidelity conditions.

Due to an error in the implementation of the force compensation, the low-fidelity conditions were repeated by the seven pilots in a second experiment session several weeks after the first session. The low-fidelity conditions without compensation (conditions 3 and 7 in Table 1) were identical between the two sessions and were used to verify that pilots performed similarly between the two sessions and assured that session was not a significant confounding variable. Comparing all dependent measures for these conditions between the two sessions revealed that pilots performed the same overall, minimizing the chances of session having a significant effect on the results.

A. Hypotheses

The hypotheses provided in Section IV.H were accepted/rejected as follows:

H1: The cutoff frequency ω_{cf} was significantly higher in the low-fidelity condition with compensation compared to without compensation for both model types and closer to that in the medium-fidelity condition. However, this trend was not detected in the RMS of the control signal RMS_u, which was similar for all low-fidelity conditions. The null hypothesis can not be fully rejected and it must be concluded that control behavior with force compensation is only more similar to that with high- or medium-fidelity motion in some respects.

H2: The compensation did not lead to an improvement in all task performance measures. Only RMS_{ye} were significantly lower with compensation. RMS_v was marginally significantly lower. We fail to reject the null hypothesis and we conclude that the control force compensation did not increase overall task performance considering both rotorcraft models at the same time.

H3: Taking into account all the RMS performance parameters in Table 2, there were little differences between the compensation and no compensation data for the UH-60. Results did not reveal a clear benefit of the force compensation with the UH-60 in low-fidelity conditions. No differences were noted in the lateral position error, lateral velocity, and roll attitude. Results showed that the RMS control input for the UH-60 was significantly lower than that of the linear model, indicating the unsteady roll rate response led to pilots staying in low-gain during the station-keeping phase. In addition, the higher force gradient for the UH-60 resulted in less control compensation relative to the linear model. This resulted in many significant interaction effects between the model and the force compensation, suggesting the null hypothesis can be rejected.

H4: Only high-fidelity motion had a much higher control input cut-off frequency than all other test conditions. Pilots performing the task under high-fidelity motion also achieved a significantly lower roll attitude and lateral velocity, which suggested pilots were able to use the motion feedback to quickly damp out the roll attitude that commanded the lateral accelerations. The RMS of control input was significantly lower in the medium-fidelity condition than in both low-fidelity conditions. The null hypothesis can not be fully rejected based on these results, i.e., high-fidelity and medium-fidelity motion do not always provide larger improvements in pilot performance compared to both low-fidelity conditions.

B. Summary

The rotorcraft model introduced significant differences in the dependent measures. These differences were probably caused by the fact that the linear model had a responsive first-order rate response, while the UH-60 model had a somewhat unsteady rate command response by purposely turning off the SAS to force pilots to stay in the loop to expose the effect of the controller compensation. This, however, might unexpectedly have led to pilots staying low-gain during the station-keeping phase. In addition, the higher force gradient of the control inceptor in the UH-60 resulted in smaller force compensations relative to the linear model with a lower force gradient. With the combination of these two factors, the benefit of having the lead provided by the force compensation was found to be significantly reduced with the UH-60 model as observed by comparing the control input cut-off frequency and lateral position error between the low-fidelity conditions with and without the force compensation.

The contrast comparing the high-fidelity condition with the rest of the fidelity conditions, and its interactions showed significant differences in the following variables: ω_{cf}, RMS_u, RMS_v, RMS_ϕ. Pilots had a higher control input cut-off frequency for the motion conditions. This might be a result of the enhanced lead information motion provides as shown by previous studies [1–5]. In this case, the simulation cueing feedback from the visual and motion were consistent with little to no phase error between them. Even though not significant, the lower RMS_u for motion conditions compared to the conditions without motion could suggest a lower control activity with motion. Furthermore, motion resulted in lower values for RMS_v and RMS_ϕ, indicating that pilots could more easily stabilize the aircraft with motion.

The medium-fidelity motion condition introduced significant differences compared to both low-fidelity conditions for t_g and RMS_u. The time-to-target t_g is lower for the medium-fidelity motion condition, even though t_g for the high-fidelity condition is not significantly different from the rest. Since the time-to-target was measuring the time of a 20-feet sidestep to the hover target, which involved taking out the lateral velocity before stabilizing and hovering, the medium-fidelity motion was able to provide the comfort for pilots to generate a larger bank, or lateral acceleration, to get to the hover target and with the right amount of damping needed to stabilize the simulator via the motion feedback.

The RMS control input RMS_u was also different for the medium-fidelity motion condition compared to the other conditions due to an interaction with the aircraft model: for the UH-60, RMS_u was significantly lower than in the low-fidelity cases, while for the linear model it was comparable to the low-fidelity conditions. This could have been caused by the UH-60's unsteady rate command system allowing motion feedback to provide the damping in the pilot's inner-loop control behavior.

The comparison between the low-fidelity condition with and without compensation found significant differences for the following variables: ω_{cf}, RMS_{ye}, RMS_v, RMS_ϕ. Even though the interaction effect is not significant ($p = 0.07$), the compensation algorithm seems to mostly increase the cutoff frequency for the linear model leaving ω_{cf} almost unchanged across the two conditions for the UH-60 model.

A significant interaction effect was found for RMS_{ye} and RMS_v: when pilots controlled the linear model, the RMS of the lateral deviation and velocity were significantly lower for the condition with compensation. On the other hand, for conditions with the UH-60 model, RMS_{ye} and RMS_v were almost unaffected across the two conditions. This is likely due to the fact that the UH-60 had an unsteady rate command response as shown in Fig. 2, resulting in pilots remaining low-gain during the station keeping phase for both low-fidelity conditions. In addition, the UH-60 had a higher force-gradient, which reduced the magnitude of the force compensation relative to the linear model. Overall, the RMS of the force compensation from all pilots was 0.155 lb_f for the linear model, and 0.107 lb_f for the UH-60.

Another interaction effect was found for RMS_ϕ: the RMS of the roll angle was significantly lower for the condition with compensation and the linear model. On the contrary, RMS_ϕ was almost unaffected between the two conditions for the UH-60. This interaction was most likely caused by the same factors as the interaction for $RMSE_{ye}$ and RMS_v.

It is apparent that the UH-60 model's response and the force gradient of the lateral stick affected pilots' approach to the task. In hindsight, a different approach to the test matrix, e.g., by using the linear model only, but varying the force gradient, might have provided more insight into the relation of pilot control behavior and task performance with motion force feedback.

VII. Conclusions

To investigate if control force compensation affects pilot control behavior and performance, pilots performed a two degrees-of-freedom lateral side-step task in the VMS under four different motion configurations (high-fidelity, medium-fidelity, low-fidelity, and low-fidelity with compensation) and with two simulated rotorcraft models (linear and UH-60 dynamics). By comparing pilots' control behavior and task performance between conditions, several conclusions could be drawn. The inertial control force compensation introduced significant differences in some of the dependent

measures, mainly for the linear model. The control input cutoff frequency was higher, the station keeping score was better, and the RMS of the lateral error was lower with compensation when no motion was present. The RMS of the lateral velocity was marginally significantly lower. Therefore, control force compensation allowed for pilot control behavior and performance more similar to that under high- or medium-fidelity motion to some extent only. Considering all performance variables, we conclude that the control force compensation did not increase overall task performance considering both rotorcraft models at the same time.

For the UH-60, the unsteady roll rate command response might have affected pilots' approach to the task and led to a low-gain control technique. In addition, the higher force gradient in the lateral stick for the UH-60 resulted in less inertial force compensation. As a result, the control force compensation only had a minimal effect on pilots' control behavior and task performance for the UH-60 model. This suggests that the control force compensation has limited benefits for controllers that have higher stiffness.

Finally, high-fidelity and medium-fidelity motion did not always provide significant improvements in pilot performance compared to the low-fidelity conditions with and without compensation.

References

[1] Sinacori, J. B., "The Determination of Some Requirements for a Helicopter Research Simulation Facility," Tech. Rep. NASA CR-152066, Systems Technology, Inc., Sep. 1977.

[2] Bray, R. S., "Visual and Motion Cueing in Helicopter Simulation," Technical Memorandum NASA TM-86818, Ames Research Center, Moffett Field (CA), Sep. 1985.

[3] Schroeder, J. A., "Helicopter Flight Simulation Motion Platform Requirements," Tech. Rep. NASA/TP-1999-208766, NASA, Jul. 1999.

[4] Stapleford, R. L., Peters, R. A., and Alex, F. R., "Experiments and a Model for Pilot Dynamics with Visual and Motion Inputs," Tech. Rep. NASA CR-1325, NASA, 1969.

[5] Jex, H. R., and Magdaleno, R. E., "Roll Tracking Effects of G-vector Tilt and Various Types of Motion Washout," *Fourteenth Annual Conference on Manual Control*, University of Southern California, Los Angeles (CA), 1978, pp. 463–502.

[6] Watson, D. C., and Schroeder, J. A., "Effects of Stick Dynamics on Helicopter Flying Qualities," *AIAA Guidance, Navigation and Control Conference*, 1990.

[7] Mitchell, D. G., Aponso, B. L., and Klyde, D. H., "Feel Systems and Flying Qualities," *AIAA Atmospheric Flight Mechanics Conference*, 1995.

[8] Lusardi, J. A., Blanken, C. L., Ott, C. R., Malpica, C. A., and von Grünhagen, W., "In Flight Evaluation of Active Inceptor Force-Feel Characteristics and Handling Qualities," *American Helicopter Society 68th Annual Forum*, 2012.

[9] Ballin, M. G., "Validation of a Real-Time Engineering Simulation of the UH-60A Helicopter," Technical Memorandum NASA TM-88360, Ames Research Center, Moffett Field (CA), Feb. 1987.

[10] Cooper, G. E., and Harper, R. P., Jr., "The Use of Pilot Rating in the Evaluation of Aircraft Handling Qualities," NASA Technical Note NASA TN D-5153, NASA, 1969.

[11] Pausder, H.-J., and Blanken, C. L., "Investigation of the Effects of Bandwidth and Time Delay on Helicopter Roll-Axis Handling Qualities," *18th European Rotorcraft Forum*, 1992.

[12] Jonckheere, A. R., "A Distribution-Free k-Sample Test Against Ordered Alternatives," *Biometrika*, Vol. 41, No. 1/2, 1954, pp. 133–145. URL `http://www.jstor.org/stable/2333011`.

[13] Laird, N. M., and Ware, J. H., "Random-Effects Models for Longitudinal Data," *Biometrics*, Vol. 38, No. 4, 1982, pp. 963–974. URL `http://www.jstor.org/stable/2529876`.

[14] Field, A., Miles, J., and Field, Z., *Discovering Statistics Using R*, Sage, 2012.